Physica Scripta. Vol. 62, 255–260, 2000

Stability and Chaos Control in Electrostatic Transducers

Y. Chembo Kouomou and P. Woafo

Laboratoire de Mécanique, Faculté des Sciences, Université de Yaoundé I, B.P. 812, Yaoundé, Cameroun

Received March 22, 1999; revised March 15, 2000; accepted March 21 2000

PACS Ref: 05.20

Abstract

In this paper, we study the dynamics of electrostatic transducers described by two nonlinearly coupled differential equations of motion. The local stability analysis of fixed points shows a transcritical bifurcation. Frequency responses and stability boundaries of oscillatory states are obtained. The system shows chaotic states and conditions for its canonical feedback control from chaos to regular orbits are derived.

1. Introduction

In recent years, various investigations have been carried out to analyse the regular and chaotic dynamics of coupled anharmonic oscillators. The interest devoted to such coupled oscillators is twofold. In the theoretical or fundamental point of view, they exhibit rich and complex behaviours. In the practical point of view, coupled non-linear oscillators describe the evolution of many biological, chemical, physical, mechanical and industrial systems (see refs. [1–5] and references therein).

Among those coupled systems, there are some for which the coupling has a non-linear character. An example of this class is the system described by the following set of non-linear differential equations

$$\ddot{x} + \lambda_m \dot{x} + x + \gamma x^3 - \alpha\left(q + \frac{1}{2}q^2\right) = F_0 \cos(\omega t), \tag{1a}$$

$$\ddot{q} + \lambda_e \dot{q} + \sigma^2(q - x - qx) = U_0 \cos(\omega t) \tag{1b}$$

where x and q are the coordinates of both oscillators, γ is a non-linearity coefficient, α and σ are coupling coefficients, λ_m and λ_e are the viscous damping coefficients. The external excitations are given by the second terms of equations (1), where F_0 and U_0 are the amplitudes, ω being the frequency. t describes the time and the dot over a variable stands for the time derivative. The coupled equations describe the motion of various mechanical engineering systems such as ships, rotating shafts, shells and composite plates [1]. Equations (1) also describe electrodynamical transducers such as electrostatic microphones and loudspeakers. The interest on such devices is justified by the fact that with the revival of the electret old idea, electrostatic microphones are widely used for various types of technological applications such as monoscope tubes for TV set signals, cassette recorders devices and evidently telephone devices [6]. To the best of our knowledge, studies carried out on electrostatic microphones and loudspeakers have been limited to linear approximations. However, their equations of motion naturally possess the non-linear terms q^2 and qx, particularly in the coupling part [6,7] and the effect of high pressure forces may cause the springs to react nonlinearly (for instance with a cubic non-linear term γx^3). Moreover, due to recent progress on the way of using chaos in engineering and technological applications, one may need to use chaos generating non-linear components in electrostatic transducers (non-linear springs and non-linear electrical components). It is therefore interesting to consider the behaviour of the devices in the non-linear limit. In the paper, we analyse the case with $U_0 = 0$ and $F_0 \neq 0$, e.g. the transducer working as a microphone.

In our first attempt on the problem, we recently used the method of multiple time scales to find amplitudes of oscillations in the resonant and non-resonant cases. We also obtained bifurcation diagrams showing period-doubling and torus breakdown routes to chaos [3].

Our aim in this paper is twofold: analysis of the stability of fixed points and that of oscillatory states – control of instability and chaos. The study of the stability uses Routh–Hurwitz criteria and the Floquet theory while the control is based on the conventional engineering approach using canonical feedback controllers. The paper is organised as follows. In Section 2, we first study the stability of fixed points with particular emphasis on the trivial point O (0,0,0,0). We then consider the oscillatory states of the devices around the fixed points. The amplitudes of oscillations are obtained using the Ritz method, and the Floquet theory is used to determine analytically the boundaries of the stable and unstable regions of a given oscillatory state. Section 3 deals with feedback control of unstable and chaotic states to desired goal orbits. We conclude in Section 4. The numerical simulation of the differential equations uses the fourth-order Runge–Kutta algorithm. Numerical results hereafter (in stars) refer to the results from the numerical simulation of equations (1).

2. Fixed points, harmonic oscillations and their stability

The normalised equations (1) in a convenient first order form give the following fourth-dimensional flow

$$\dot{x}_1 = x_2, \tag{2a}$$

$$\dot{x}_2 = -\lambda_m x_2 - x_1 - \gamma x_1^3 + \alpha\left(x_3 + \frac{1}{2}x_3^2\right) + F_0 \cos \omega t, \tag{2b}$$

$$\dot{x}_3 = x_4, \tag{2c}$$

$$\dot{x}_4 = -\lambda_e x_4 - \sigma^2(x_3 - x_1 - x_1 x_3) \tag{2d}$$

where $x_1 = x$, $x_2 = \dot{x}$, $x_3 = q$ and $x_4 = \dot{q}$.

In the vector notation, the flow (2) reduces to

$$\dot{u} = g(u, t) \tag{3}$$

with

$$u = u(x_1, x_2, x_3, x_4).$$

In the analysis which follows in this section 2, we first analyse the stability of fixed points (autonomous model) in the natural state where the cubic term γx_1^3 is neglected (section 2.1). Then follows in section 2.2 the stability of harmonic oscillations around fixed points (with γx_1^3 still discarded). Finally, in section 2.3, we consider the whole model equations to analyse the effects of the cubic term on the behaviour of the system.

2.1 *Fixed points and their stability*

The fixed points satisfy $g(u) = 0$. One can easily find that the model possesses three fixed points, which are

$$u_{01} = (0, 0, 0, 0),\ u_{02} = (x_{02}, 0, q_{02}, 0),\ u_{03} = (x_{03}, 0, q_{03}, 0). \tag{4}$$

where

$$x_{02} = 1 - \alpha\frac{1 + \sqrt{1 + \frac{8}{\alpha}}}{4}, \quad q_{02} = \frac{-3 + \sqrt{1 + \frac{8}{\alpha}}}{2},$$
$$x_{03} = 1 - \alpha\frac{1 - \sqrt{1 + \frac{8}{\alpha}}}{4}, \quad q_{03} = \frac{-3 - \sqrt{1 + \frac{8}{\alpha}}}{2}.$$

The local stability analysis of fixed points u_{0i} can be determined by investigating the linearilized system

$$\dot{u} = J(u_{0i}) \cdot u, \tag{5}$$

where $J(u_{0i})$ is the Jacobian of g at u_{0i}. The characteristic equation of the Jacobian matrix is then written as:

$$s^4 + (\lambda_m + \lambda_e)s^3 + (\lambda_m\lambda_e + \sigma^2(1 - x_{0i}) + 1)s^2 + (\lambda_e + \lambda_m\sigma^2(1 - x_{0i}))s + \sigma^2((1 - x_{0i}) - \alpha(1 + q_{0i})^2) = 0. \tag{6}$$

From the classical local stability analysis of Lyapunov, it is known that the fixed points are stable if the real parts of the roots of the characteristic equation (6) are all negative. Otherwise (if at least one root has a positive real part), the fixed point is unstable. Using Routh–Hurwitz criterion [8] for the sign of the real part of roots, we obtain that the stability of both u_{01} and u_{02} depend only on the quantity α which defines the ratio between electrostatic and mechanical energies. Moreover, we find that an exchange of stability occurs at $\alpha = 1$. Indeed, for $\alpha < 1$, the equilibrium point u_{01} is stable while u_{02} is unstable, and for $\alpha > 1$, u_{01} is unstable while u_{02} is stable. Thus, $\alpha = 1$ corresponds to a transcritical bifurcation point [9]. The stability of the fixed point u_{03} depends on α, G and the damping coefficients λ_m and λ_e, but it can not be investigated analytically.

2.2 *Harmonic oscillations and their stability*

Due to the complexity of the coupled equations, it is difficult to find analytical forms for a general solution of oscillatory states which takes into account the effects of the quadratic non-linearity. An attempt to achieve that goal was considered in ref. [3] where we used the method of multiple time scales to analyse the behaviour of the system in the resonant and non resonant cases. Here, we are interested by the amplitudes and stability of the forced oscillations around the fixed points u_{0i} $(i = 1, 2)$. For this aim, we assume that the responses of the system (around its fixed points) to external sinusoidal excitations are defined as

$$x_h = x_{0i} + A\cos(\omega t - \varphi), \tag{7a}$$
$$q_h = q_{0i} + B\cos(\omega t - \phi). \tag{7b}$$

A and B are the amplitudes of oscillations while φ and ϕ define the phases with respect to the external excitations. Inserting (7a) and (7b) in equation (1) and making use of the classical Ritz variational method, we obtain

$$A^2 = \frac{[\lambda_e^2\omega^2 + (\sigma^2(1 - x_{0i}) - \omega^2)^2]F_0^2}{\Delta}, \tag{8a}$$
$$B^2 = \frac{[\sigma^4(1 + q_{0i})^2]F_0^2}{\Delta}, \tag{8b}$$
$$\varphi = \mathrm{Arc}\tan\left(\frac{\Delta_1}{\Delta_3}\right), \tag{8c}$$
$$\phi = \mathrm{Arc}\tan\left(\frac{\Delta_2}{\Delta_4}\right) \tag{8d}$$

where

$$\Delta_1 = [(\sigma^2(1 - x_{0i}) - \omega^2)][\lambda_m(\sigma^2(1 - x_{0i}) - \omega^2) + \lambda_e(1 - \omega^2)]\omega - \lambda_e\omega[(1 - \omega^2)(\sigma^2(1 - x_{0i}) - \omega^2) - \lambda_e\lambda_m\omega^2 - \alpha\sigma^2(1 + q_{0i})^2], \tag{9a}$$

$$\Delta_2 = [\lambda_m(\sigma^2(1 - x_{0i}) - \omega^2) + \lambda_e(1 - \omega^2)]\omega, \tag{9b}$$

$$\Delta_3 = [(\sigma^2(1 - x_{0i}) - \omega^2)][(1 - \omega^2)(\sigma^2(1 - x_{0i}) - \omega^2) - \lambda_e\lambda_m\omega^2 - \alpha\sigma^2(1 + q_{0i})^2] + \lambda_e\omega^2[\lambda_m(\sigma^2(1 - x_{0i}) - \omega^2) + \lambda_e(1 - \omega^2)], \tag{9c}$$

$$\Delta_4 = [(1 - \omega^2)(\sigma^2(1 - x_{0i}) - \omega^2) - \lambda_e\lambda_m\omega^2 - \alpha\sigma^2(1 + q_{0i})^2] \tag{9d}$$

and

$$\Delta = [(1 - \omega^2)(\sigma^2(1 - x_{0i}) - \omega^2) - \lambda_e\lambda_m\omega^2 - \alpha\sigma^2(1 + q_{0i})^2]^2 + \omega^2[\lambda_m(\sigma^2(1 - x_{0i}) - \omega^2) + \lambda_e(1 - \omega^2)]^2. \tag{9e}$$

It should be noted that for $x_{0i} = q_{0i} = 0$, the above harmonic solution reduces to what can be obtained in the linear limit. In Figure 1, we have plotted the amplitudes A and B as functions of ω and α. Figure 1a shows the well known anti-resonant phenomena. Figure 1b presents the variation of A as function of α. It is seen that the amplitudes for $\alpha < 1$ and $\alpha > 1$ coalesce at $\alpha = 1$ (ie they have the same value at the transcritical point $\alpha = 1$).

An interesting matter related to an oscillating solution is the analysis of its stability. In particular, for the electrostatic transducer considered, it is of practical interest to know how the quadratic non-linearity (always neglected) affects the stability of the harmonic solutions described above. For this aim, consider the variational equations of (1) around solutions (7):

$$\delta\ddot{x} + \lambda_m\delta\dot{x} + \delta x - \alpha(1 + q_h)\delta q = 0, \tag{10a}$$
$$\delta\ddot{q} + \lambda_e\delta\dot{q} + \sigma^2(1 - x_h)\delta q - \sigma^2(1 + q_h)\delta x = 0 \tag{10b}$$

where δx and δq are perturbations of x_h and q_h respectively.

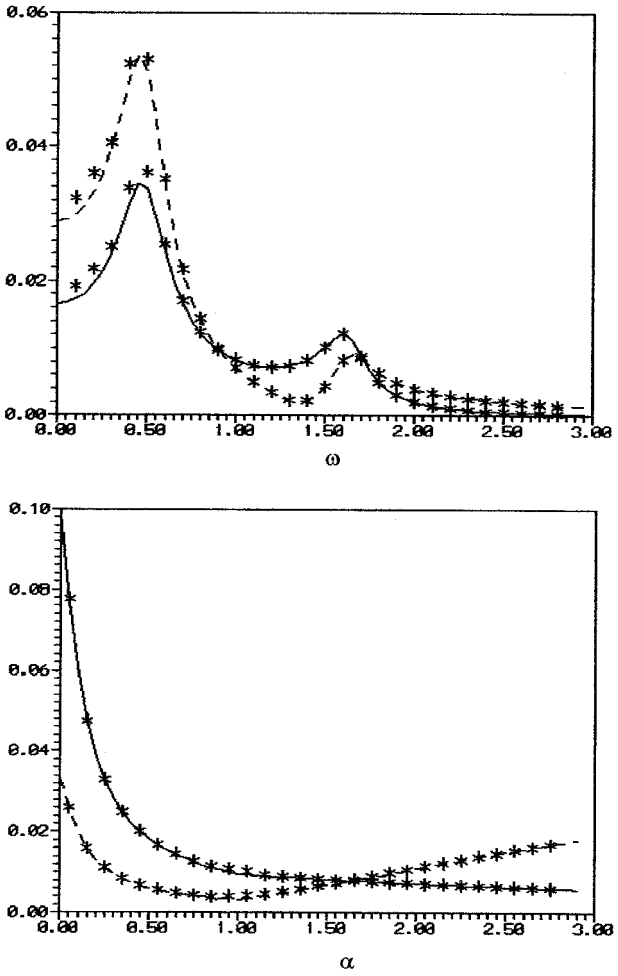

Fig. 1. (a) Frequency responses without cubic non-linearity for oscillations around the fixed point u_{02} with $\alpha = 1.5$; $\sigma = 1.2$; $\lambda_m = 0.3$; $\lambda_e = 0.2$; $F_0 = 0.01$. (Full line for B and dash for A, stars for numerical results). (b) Variation of A and B as functions, of the parameter α with $\sigma = 1.2$; $\lambda_m = 0.3$; $\lambda_e = 0.2$; $F_0 = 0.01$; $\omega = 1$. (Full line for B and dash for A, stars for numerical results).

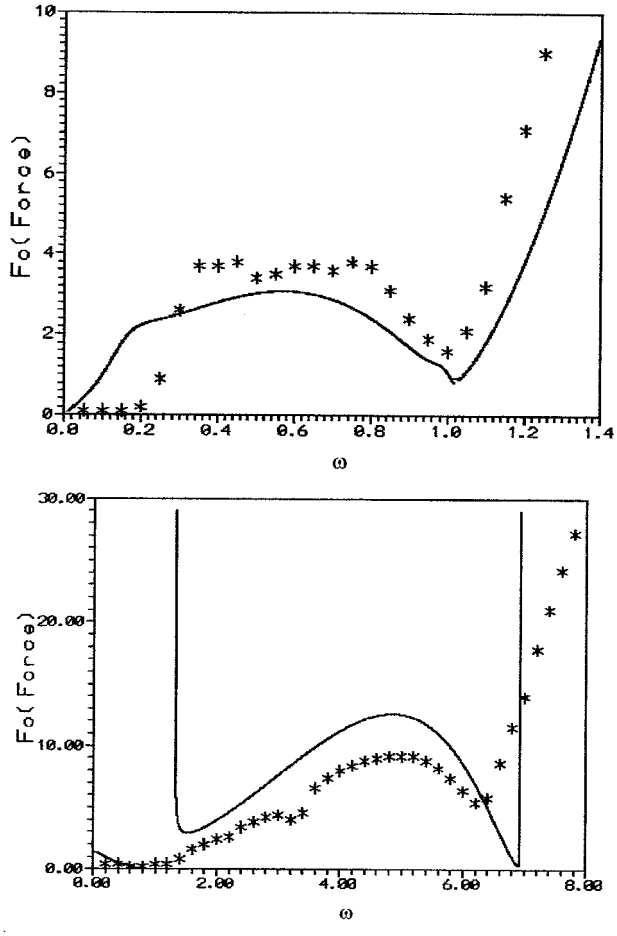

Fig. 2. (a) Stability boundary in the ω-F_0 plane with $\alpha = 1.0$; $\sigma = 0.2$; $\lambda_m = 0.1$; $\lambda_e = 0.3$. (Full line for analytical boundary and stars for numerical results). (b) Same as fig. 2a with $\alpha = 2.5$; $\sigma = 5.0$; $\lambda_m = 0.2$; $\lambda_e = 0.1$. (Full line for analytical boundary and stars for numerical results).

The solution (7) is stable if δx and δq remain bounded as the time tends to infinity. The problem can be tackled using Floquet theory [1,8]. By considering the lower-order Hill determinant of the equations (a 6th order determinant), it is found that the hypersurface delimiting stable and unstable regions is described by the following equation

$$\Delta(\xi_m, \xi_e) = \begin{vmatrix} \delta_{11}-4 & 0 & +4\xi_m & \delta_{12} & 2\gamma_{12} & 0 \\ 0 & \delta_{11} & 0 & \gamma_{12} & \delta_{12} & \theta_{12} \\ -4\xi_m & 0 & \delta_{11}-4 & 0 & 2\theta_{12} & \delta_{12} \\ \delta_{21} & 2\gamma_{21} & 0 & \delta_{22}-4 & 2\gamma_{22} & +4\xi_e \\ \gamma_{21} & \delta_{21} & \theta_{21} & \gamma_{22} & \delta_{22} & \theta_{22} \\ 0 & 2\theta_{21} & \delta_{21} & -4\xi_e & 2\theta_{22} & \delta_{22}-4 \end{vmatrix} = 0 \tag{11}$$

where the δ_{ij} (which are not Kronecker symbols, we emphasise), γ_{ij}, θ_{ij}, ξ_m and ξ_e coefficients are all defined in appendix I.

Figures 2a and 2b show two stability boundaries in the (ω, F_0) plane for sets of the system parameters. In stars, we have depicted results of the same stability boundary obtained from a direct numerical study of the equations of motion (1).

Let us note that in Figure 2b, the analytical curve possesses two branches for low frequencies. In both figures, we observe an agreement between the analytical prediction of the Hill determinant and those of the numerical calculations for low frequencies. For high frequencies, the separation between the results and the numerical results is large. We expect that the separation can be reduced if we increase the order of the Hill determinant.

2.3 *Effects of the cubic terms on the behaviour of the system*

If the springs have a non-linear character, new interesting phenomena can appear. But because of the complexity of the resulting equations of motion, we only concentrate on the analysis of symmetrical harmonic oscillations around the fixed point (0,0,0,0). Thus considering solutions of the form (7) with $x_{0i} = q_{0i} = 0$, and making use as before of the Ritz procedure, we find that the amplitude A of the dimensionless displacement x satisfies the following nonlinear algebraic equation

$$\left[\left[(1-\omega^2)+\frac{3}{4}\gamma A^2\right] - \frac{\alpha\sigma^2(\sigma^2-\omega^2)}{(\sigma^2-\omega^2)^2+\lambda_e^2\omega^2}\right]^2 A^2 + \left[\lambda_m\omega + \frac{\alpha\sigma^2\lambda_e\omega}{(\sigma^2-\omega^2)^2+\lambda_e^2\omega^2}\right]^2 A^2 = F_0^2. \tag{12}$$

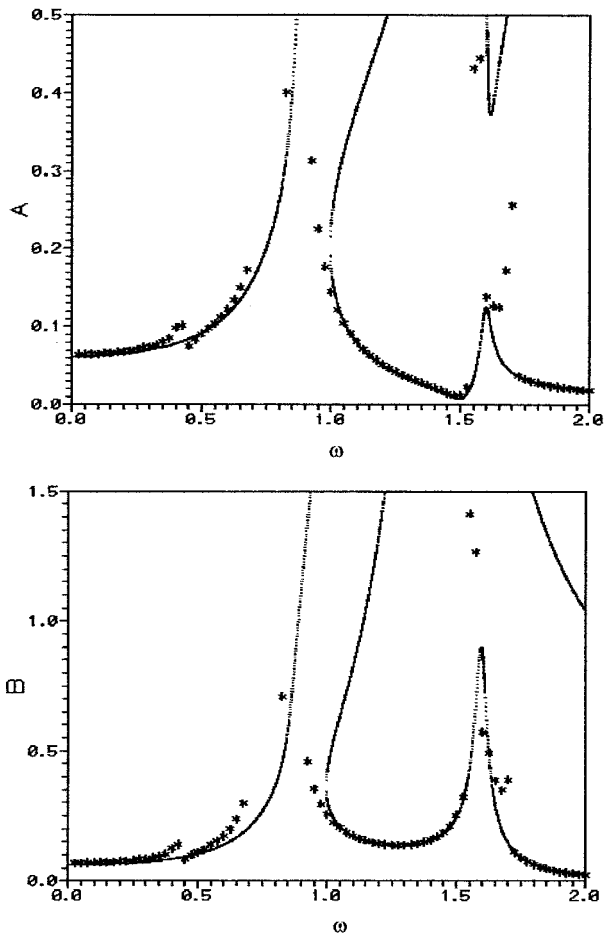

Fig. 3. Frequency responses $A(\omega)$ (Fig. 3a) and $B(\omega)$ (Fig. 3b) considering the cubic non-linearity with $\alpha = 0.2$; $\sigma = 1.5$; $\lambda_m = 0.01$; $\lambda_e = 0.05$; $\gamma = 0.6$; $F_0 = 0.05$. (Stars for the numerical simulation).

The amplitude B of the dimensionless charge q is related to A by

$$B = \frac{\sigma^2 A}{\sqrt{(\sigma^2 - \omega^2)^2 + \lambda_e^2 \omega^2}}. \tag{13}$$

Figures 3a and 3b show the frequency responses $A(\omega)$ and $B(\omega)$. Superimposed on the plots are the results (in stars) obtained from a direct numerical simulation of the equations of motion (1). The initial conditions are (0,0,0,0).

As it appears in Figure 3, there are qualitative and quantitative disagreements between the analytical results and the numerical results. Indeed, the numerical simulation indicates various jump phenomena at $\omega = 0.4$ and 0.72 (this does not appear in the analytical results). Resonance occurs at $\omega \cong 0.75$ and $\omega \cong 1.5$. This corresponds to states where the second oscillator (q) enters into resonance ($\omega = \sigma$) and subharmonic resonance ($\omega = \sigma/2$) with the external excitation. These resonant states can be obtained analytically using for instance the multiple scale method [1, 3]. We can also notice that for few intervals (for example $0.68 < \omega < 0.84$), the external frequency induces unstable oscillatory states.

3. Chaotic states and canonical feedback control

3.1 *Chaotic states*

During our numerical simulations, it has appeared that the coupled equations (1) can lead to complex dynamical behaviours such as multiperiodic, quasiperiodic and chaotic states. This has already been reported in our ref. [3]. We have also noticed that without the cubic non-linearity γx^3, the system does scarcely show chaotic behaviour. It is also found that there are various routes to chaos (such as sudden transition and torus breakdown or quasiperiodic route) with several kinds of periodic and multiperiodic windows. A typical bifurcation diagram is illustrated in Figure 4 where the coordinate x in the Poincaré map is plotted versus σ. Similar or other types of bifurcations can be obtained for other sets of parameters, or by varying another parameter (for instance α or F_0).

As any natural phenomena, and depending on the context and the usage, the presence of chaos in natural and man-made devices can be considered as a positive or negative issue. In fact, in many situations, chaos is undesirable since it leads to irregular performance and possible catastrophic failures. In this case, it should be suppressed or controlled. But in some other cases, chaos appears to be a beneficial feature such as in mechanical heat and transport phenomena [10]. Serious progress in the way of using chaos to secure communication [11] has also been made recently. Moreover, nowadays, intensive research is carried out to discuss the wide variety of applications of chaos in various fields ranging firom natural, physical, engineering and social sciences. It is in this spirit that we expect that the presence of chaos in an electrostatic transducer serving as microphone and loudspeaker can be useful both in its irregular structure or in a regular structure obtained after the control.

3.2 *Canonical feed-back control of chaos*

As concerns the control, increasing interest has been devoted to the subject using mainly feedback and non feedback methods [see for instance refs. [12–16] and references therein]. But let us note that the literature on the subject is still growing. The control aims at suppressing chaos or take advantage of the various infinite number of different

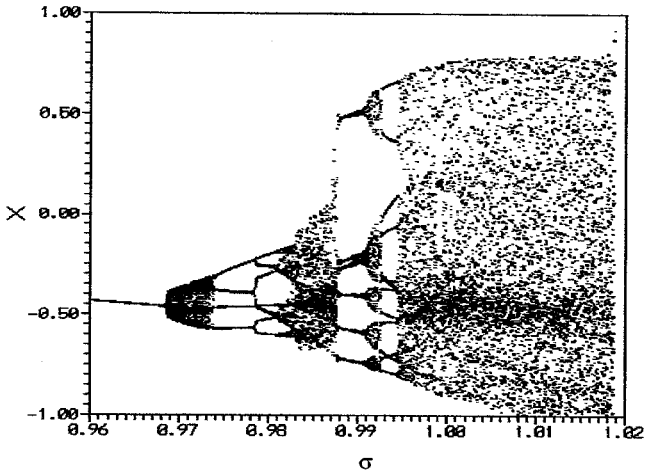

Fig. 4. Bifurcation diagram with $\alpha = 0.1$; $\lambda_m = 0.03$; $\lambda_e = 0.30$; $\gamma = 1.0$; $\omega = 1.0$; $F_0 = 0.7$.

unstable orbits embedded in the chaos attrattor to tune the system to a large number of distinct and desired periodic orbits.

In ref. [14], the conventional engineering approach of automatic control using canonical feedback controllers has been used to direct a Duffing oscillator from a chaotic trajectory to one of its periodic or multiperiodic orbits. We extend the approach to the coupled equations of motion of the electrostatic transducers.

Let us assume that the target trajectory in four dimensional space is $\bar{u} = (\bar{x}_1, \bar{x}_2, \bar{x}_3, \bar{x}_4)$ in the sense that $u(t)$ (see eq. (3)) tends to $\bar{u}$ after the control has been applied on eq. (2) or on eq. (3). The conventional feed-back controller has the form

$$\mathbf{C} = -[\mathbf{K}_{ij}](u - \bar{u}), \tag{14}$$

where $[\mathbf{K}_{ij}]$ is a 4×4 feedback gain matrix ($i = 1$ to 4 and $j = 1$ to 4). Theoretically, this gives sixteen degrees of freedom which can be used to ensure the control. The resulting control equation then becomes

$$\dot{u} = g(u, t) - [\mathbf{K}_{ij}](u - \bar{u}) = \mathbf{g}_c(u, t), \tag{15}$$

where $\mathbf{g}_c(u, t)$ is a four dimensional vector function including the components of the original equation as well as those due to the controller. For the controller system to be stable, it is required that the characteristic equation of the 4×4 Jacobian matrix

$$\mathbf{J}_c = \left[\frac{\partial \mathbf{g}_{ci}}{\partial x_j}\right] \tag{16}$$

at $\bar{u}$ has all its roots located in the left-half of the complex plane. The characteristic equation reads

$$s^4 + a_1 s^3 + a_2 s^2 + a_3 s + a_4 = 0 \tag{19}$$

with

$$a_1 = \lambda_m + \lambda_e,$$
$$a_2 = \lambda_m \lambda_e + (1 + 3\gamma \bar{x}^2 + K_{21}) + (K_{43} + \sigma^2(1 - \bar{x})),$$
$$a_3 = \lambda_e(1 + 3\gamma \bar{x}^2 + K_{21}) + \lambda_m(K_{43} + \sigma^2(1 - \bar{x})),$$
$$a_4 = (1 + 3\gamma \bar{x}^2 + K_{21})(K_{43} + \sigma^2(1 - \bar{x})) - \alpha\sigma^2(1 + \bar{q})^2.$$

The Routh–Hurwitz criteria gives four inequalities involving the components $\mathbf{K}_{ij}$, the system parameters and the target components $\bar{x}_1$, $\bar{x}_2$, $\bar{x}_3$, and $\bar{x}_4$. Let us assume for simplicity that except the components K_{21} and K_{43}, all the other components of the feedback gain matrix are suppressed (set equal to zero). The above analysis leads to the following condition for the control

$$\mathbf{K} > \frac{-[\mu(1 + 3\gamma \bar{x}_{\min}^2) + \sigma^2(1 - \bar{x}_{\max})] + \sqrt{[\mu(1 + 3\gamma \bar{x}_{\max}^2) - \sigma^2(1 - \bar{x}_{\max})]^2 + 4\mu\alpha\sigma^2(1 + \bar{q}_{\max})^2}}{2\mu}$$

where $\bar{x}_{\min}$, $\bar{x}_{\max}$ and $\bar{q}_{\max}$ are extremal values of the periodic displacement and charge targets.

We have assumed $K_{21} = K$, and $K_{43} = \mu K$, with $\mu, K > 0$.

Let us consider the dynamics of the uncontrolled system with following set of parameters:

$\lambda_m = 0.03$; $\lambda_e = 0.30$; $\alpha = 0.1$; $\sigma = 1.0$; $\gamma = 1.0$; $F_0 = 0.7$ and $\omega = 1.0$.

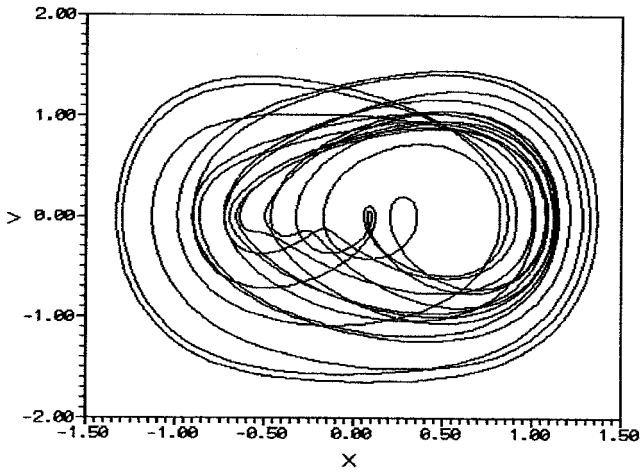

Fig. 5. Chaotic response for $\alpha = 0.1$; $\sigma = 1.0$; $\lambda_m = 0.03$; $\lambda_e = 0.30$; $\gamma = 1.0$; $\omega = 1.0$; $F_0 = 0.7$.

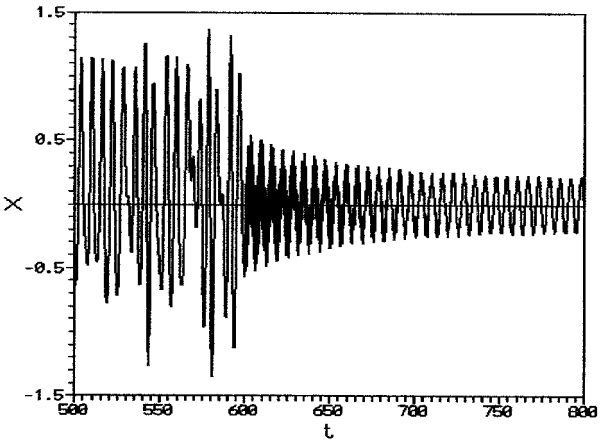

Fig. 6. Controlling the chaotic response of Fig. 5 to the target orbit.

As it appears in the bifurcation diagram of Figure 4 and also in Figure 5, this set of parameters leads the system to a chaotic state. To test the validity of the control condition (18), we have considered as a target state the following periodic oscillation

$$\bar{x}(t) = 0.2 \cos \omega t \quad \text{and} \quad \bar{q}(t) = 0.2 \cos \omega t. \tag{19}$$

In the numerical simulation, the control gain components $K_{21} = K_{43} = 50$ show how the control tunes the system from the chaotic states to the desired orbit (Figure 6). A similar figure can be drawn for the q component of the system.

4. Conclusion

In this paper, we have considered the problem of stability of fixed points and oscillatory states, and the problem of chaos control in an electrostatic transducer. This transducer can serve as a microphone or as a loudspeaker. The local stability analysis of fixed points has led to a transcritical bifurcation. For the oscillatory states around fixed points, frequency responses have been obtained and their stability diagram plotted from the Floquet theory and from a direct numerical simulation of the equations of motion.

When a cubic non-linearity is added to the system as a consequence of the non-linear behaviour of the spring,

the frequency response for harmonic solution shows the well known jump phenomena. Moreover, the system exhibits complex dynamical behaviours such as multiperiodic, quasiperiodic and chaotic responses. The transition to chaos follows various routes. A discussion on the usefulness of chaos in electrostatic transducers is presented. Finally, we have derived conditions for the canonical feedback control of the system from chaotic states to desired regular goal dynamics.

The analysis carried out in this paper can be extended to other electromechanical or electroacoustical devices. Furthermore, it is worth mentioning that a possible practical implementation of the chaos control design is of technological interest and will be welcome. Beyond these points which we think deserve investigations, there is another interesting problem related to electrostatic transducers. It consists of the excitation of the device by noises. This problem is also currently under investigation.

Appendix: Coefficients of equation (11)

The δ_{ij} coefficients are defined by

$$\delta_{11} = \frac{4}{\omega^2}; \quad \delta_{12} = -\frac{4\alpha(1+q_{0i})}{\omega^2}; \quad \delta_{21} = -\frac{4\sigma^2(1+q_{0i})}{\omega^2};$$

$$\delta_{22} = \frac{4\sigma^2(1-x_{0i})}{\omega^2}.$$

γ_{ij} and θ_{ij} can be written as

$$\gamma_{11} = 0; \quad \gamma_{12} = -\frac{2\alpha B}{\omega^2}\cos\phi; \quad \gamma_{21} = -\frac{2\sigma^2 B}{\omega^2}\cos\phi;$$

$$\gamma_{22} = -\frac{2\sigma^2 A}{\omega^2}\cos\varphi.$$

$$\theta_{11} = 0; \quad \theta_{12} = -\frac{2\alpha B}{\omega^2}\sin\phi; \quad \theta_{21} = -\frac{2\sigma^2 B}{\omega^2}\sin\phi;$$

$$\theta_{22} = -\frac{2\sigma^2 A}{\omega^2}\sin\varphi,$$

where A, B, φ and ϕ are defined in equations (8).

We also have

$$\xi_m = \frac{\lambda_m}{\omega}; \quad \xi_e = \frac{\lambda_e}{\omega}.$$

At last we note that in our calculations, we have used the fixed point (x_{01}, q_{01}) for $0 < \alpha \leq 1$ and the fixed point (x_{02}, q_{02}) for $\alpha \geq 1$.

References

1. Nayfeh, A. H. and Mook, D. T., in "Nonlinear Oscillations" (John Wiley and Sons, New-York, 1979).
2. Woafo, P., Chedjou, J. C. and Fotsin, H. B., Phys. Rev. **E54**, 5929 (1996).
3. Woafo, P., Fotsin, H. B. and Chedjou, J. C., Physica Scripta **57**, 195 (1998).
4. Landa, P. S. and Rosenblum, M. G., Appl. Mech. Rev. **46**, 414 (1993), Pikovsky, A., Rosenblum, M. and Kurths, J., Europhys. Lett. **34**, 165 (1996), Kozłowski, J., Parlitz, U. and Lanterborn, W., Phys. Rev. **E51**, 1861 (1995).
5. Kapitaniak, T. and Steeb, W. H., Phys. Lett. **A152**, 33 (1991), Pastor-Diaz, I. and López-Fraguas, S. A., Phys. Rev. **E52**, 1480 (1995).
6. Sinclair, I. R., in "Sensors and Transducers", 2nd edition (Butterworth-Heinemann, 1992).
7. Lehmann, R., in "Les Transducteurs Electro et Mécano-Acoustiques. Haut-parleurs et Microphones" (Chiron, Paris, 1963), Rocard, Y., in "Dynamique des Vibrations" (Gauthier-Villars, Paris, 1960), Mathieu, J. P., in "Vibrations et Phénomènes de Propagation", Vol 1 (Masson Cie, Paris, 1974).
8. Hayashi, C., in "Nonlinear Oscillations in Physical Systems" (Mc-Graw-Hill, New-York, 1964).
9. Wiggins, S., in "Introduction to Applied Nonlinear Dynamical Systems and Chaos" (Springer-Verlag, 1990).
10. Ottino, in "Kinematics of Mixing: Stretching, Chaos and Transport" (Cambridge University Press, Cambridge, 1989).
11. Pecora, L. M. and Carrols, T. L., Phys. Rev. Lett. **64**, 821 (1990), Hayes, S., Grebogi, C., Ott, E. and Mark, A., Phys. Rev. Lett. **73**, 1781 (1994), Cuomo, K. M. and Oppenheim, A. V., Phys. Rev. Lett. **71**, 65 (1993), Perez, G. and Cerdeira, H. A., Phys. Rev. Lett. **44**, 1970 (1995), Boccaletti, S., Farini, A. and Arechi, F. T., Phys. Rev. **E55**, 4979 (1997).
12. Ott, E., Grebogi, C. and Yorke, Y. A., Phys. Rev. Lett. **64**, 1196 (1990).
13. Pyragas, K., Phys. Lett A **170**, 421 (1992).
14. Chen, G. and Dong, X., IEEE Trans. Circuits Syst. I **40**, 591 (1993).
15. Paul Raj, S. and Rajasekar, S., Phys. Rev. **E55**, 6237 (1997).
16. Kapitaniak, T., "Controlling Chaos", (Academic Press, London, 1996).